

Influence of Brownian motion and viscous dissipation on Jeffrey Ternary-Hybrid Nanofluid Flow on an Unsteady Stretching Surface with Thermophoresis

¹M Annapoorna,

Degree Lecturer, Department of Mathematics, TSWRDCW, Telangana, India.

²Dr.E.Rama,

Associate Professor, Department of Mathematics, Osmania University, Hyderabad, India.

*Corresponding author: annapura.mogilipaka@gmail.com

Abstract

This research aims to analyze the influence related to viscous dissipation and Brownian motion on Jeffrey ternary-hybrid nanofluid flow upon an unsteady moving surface along mixed convection and thermophoresis. The surface mass flux is also regarded to be zero so that the nanoparticle fraction is preserved in the presence of a very large obstruction. Similarity transformations are used to change the governing non-linear PDEs in the direction of ODEs, which can be solved through numerical calculations via the shooting technique and the fourth-order R.K. integration scheme. The different graphical results are reviewed in detail with different parameters used. The staggering effect of related constraints on heat and velocity curves is inspected by varied schemes. The computational data for the skin friction coefficient and heat transfer rate are also graphically mentioned. It was found from the graphical results show that when Deborah's number and Hartmann's number decrease, the velocity curves rise, and as the mixed convection parameter increases, the velocity curves fall. Eckert number, Deborah number, Hartmann number, and mixed convection parameters have been detected to reveal the temperature profile. Ternary hybrid nanoparticles are especially susceptible to these phenomena. The increased Brownian motion of ternary hybrid nanoparticles results in a higher temperature because of the transformation of kinetic energy to heat energy. Concentrations of ternary nanofluids are enhanced by increasing the thermophoresis parameter. Because of the higher fluid density, the skin friction value for the Eckert number increased.

Keywords: Ternary hybrid nanofluid; Jeffrey fluid; Brownian motion; viscous dissipation.

1. Introduction

Suspension of nanoparticles in conventional base fluids is got great interest to investigators and scientists because of the special thermal performance in several branches of the engineering disciplines. Excellent performance by nanofluids was outstanding and led to successful results in the phenomenon of heat transfer, which alerted scientists to work on different groups of nanoparticles known as "hybrid nanofluids". From the experiments, it was discovered that the heat transfer rate of the hybrid nanofluid is greater than the heat transfer rate of the monolithic nanofluid. El-Zahar et al. [1] used the nanofluid to investigate the effect of Brownian motion and viscous dissipation over Jeffrey flow on an unstable moving surface using mixed convection and thermophoresis. Ramzan et al. [2] used differently shaped Al_2O_3 particles with the base liquid to confirm the thermophysical properties of thermal transfer of an unstable thin film flow across an extended surface across convective boundary conditions and they found that Al_2O_3 nanoparticles possessed high heat transfer. Aybar et al. [3] added tiny particles into a fluid known as base fluid. Therefore, for each basic fluid, its heat conduction is raised. As an illustration, we can rely on Akbar et al. [4] for the heat

conductivity of nanofluids, different models have been studied, Such as Hamilton and Croeser are among the most widely used models for heat conductivity models about nanofluids. Akbar et al. [4] Researchers looked at how different nanoparticles performed in terms of heat transfer and continued [5] to talk about how heat radiation and different thermal conductivities affect the elongation layer. They then looked into the numerical analysis of the transmission of magnetohydrodynamic nanofluids through an expansion plate. [6]. We may discuss diverse aspects of nanofluid flow [7] & [8]. Manzoor et al. [9] investigated the 3-D unstable flow of the second-order nanofluid through thermal electrophoresis and under the impact of Brownian motion (Nb). They observed that the temperature & nanomaterials should be reduced to reduce higher values of the instability coefficient. Faizan et al. [10] research on a nonlinear system of PDEs in a cylindrical axis was created using the Buongiorno method to investigate the role of wall stress and heat transfer rate in the unstable shear behaviour of nanofluid flow on an exponentially expanding and contracting cylinder. Yun-Xiang et al. [11] used the biotransformation flow of a magnetic Maxwell nanomaterial through an extended cylinder under the effects of slip. They analyzed the flow by encountering the new activation energy and thermal radiation features. Jie Liu et al. [12] used an unstable Casson nanofluid along a radiant extended surface with a stagnation point dependent on the load condition and heat source, they noted that the increasing values of Brownian motion coefficient increase and decrease Sherwood number, fluid concentration, and Schmidt number, and conversely, the thermal transfer coefficient increases. Khan et al. [13] applied the third-order fluid model to discuss the behaviour of a non-Newtonian fluid through buoyancy flows and an extended permeable surface. Additionally, Freidoonimehr et al. [14]. dealt with a nanofluid's free convective laminar movement under the influence of a magnetic field in a porous media moving along a vertically extended surface.

Recent studies have shown that nanofluids have a much larger impact on the heating capacity of an object than ordinary fluids. The suspending of nanomaterials enhances the transmission of the heat capacity of the working fluids, and hence it improves the thermophysical characteristics that make the object more efficient. Then nanofluids and their effects on advanced technology and scientific knowledge have shown rewarding results that encourage investigators to consider the thermophysical characteristics of nanofluids. The suspending of one nanoparticle has no special applications in industrial and engineering problems, so it is not sufficient for the required thermal efficiency. Therefore, a "hybrid nanofluid" is applied. By Makishima [15] a hybrid nanofluid is created through involves combining two or more nanoparticle types into a single base fluid. Different cooling systems, thermal generators, and engineering issues have all benefited from the increased efficiency of heat transmission that hybrid nanofluids provide. Sarkar et al. [16] observed that compared to monolithic nanofluids, hybrid nanofluids have superior thermal conductivity and pressure loss properties. Hybrid nanofluids have been used by numerous scientists and scholars due to their excellent heat transfer capabilities. Wakeef et al. [17] used the application of mixed Al_2O_3 and CuO nanofluids to study their effect on surface roughness and thermal radiation using Buongiorno's generalized nanofluidic model. Seddik et al. [18] examined the preparation methodology, and the strength of the hybrid nanocomposite and explained the uses of hybrid nanofluids in current technology and science. The strength and thermophysical characteristics of hybrid nanofluids were investigated, and Xian et al. [19] reported some advanced properties. Both Kazmi et al. [20] and Soltani et al. [21], who conducted experimental research into the effect of the hybrid nanofluid, found that the working fluids exhibited a significantly different rate of heat transmission when the nanofluid was present. X. Sun et al. [22] discussed the importance of the nanoparticle size, water-transporting copper nanoparticles, and spatially-dependent heating. Sabu et al. [23] looked into the structure of the nanoparticles over the flow of a MHD Al_2O_3 nanofluid on a heated turntable.

Dawar et al. [24] researched the impact of MHD on a nanoflux model in a thin iron oxide that has a rotational tilt based on sodium alginate revealed to incident solar energy. Wenhao et al. [25] addressed the effect of three-way hybrid nanofluids on the motion of a colloidal solution and found that increasing the three distinct nanoparticles moved at random. Manjunatha et al. [26] found that more heat is generated by the ternary-hybrid nanofluid as well as increased flow momentum for the larger volume fraction. Xian et al. [27] found that graphene-based ternary hybrid nanofluids, unlike Newtonian performance at greater concentrations, exhibited the features of the shear-thinned fluid at low concentrations through the study of two dehydrated water-deionized ternary-hybrid nanofluids. Muhammad et al. [28] analyzed the impact of ternary hybrid nanofluids on the water with different forms of nanoparticles, and the Observations revealed that the use of water-based triple-hybrid nanofluids increases the rate of heat transmission.

The main goal of this research relates to modelling the influence of Brownian motion (Nb) and viscous dissipation on Jeffrey's ternary-hybrid nanofluid flow upon an unsteady moving surface with thermophoresis. Given that thermophoresis-assisted flow of Jeffrey ternary-hybrid nanofluids across an unsteady stretchy surface is not discussed elsewhere. Additionally, the roles of the ternary-hybrid nanofluid parameters, Deborah, and Eckert numbers were computationally submitted.

2. Mathematical Model

We considered a magneto-mixed convection Jeffrey ternary-hybrid nanofluid flow upon an unsteady moving surface. By considering thermophoresis and dissipation effects, we discussed the characteristics of Brownian motion. Since we assume no mass flux of nanoparticles, we can use a constant magnetic strength B_0 , applied perpendicular to the surface. The concentration distribution is C_∞ , whereas the ambient temperature field persists at T_∞ , and the constant temperature at the surface is T_w . The governing equations that regulate the fluid flow are given by [1]

$$\frac{\partial u}{\partial x} + \frac{\partial v}{\partial y} = 0 \tag{1}$$

$$\frac{\partial u}{\partial t} + u \frac{\partial u}{\partial x} + v \frac{\partial v}{\partial y} = \frac{\nu_{Thnf}}{(1+\lambda_2)} \left\{ \frac{\partial^2 u}{\partial y^2} + \lambda_1 \left(\frac{\partial^3 u}{\partial y^2 \partial t} + u \frac{\partial^3 u}{\partial y^2 \partial x} - \frac{\partial u}{\partial x} \frac{\partial^2 u}{\partial y^2} + \frac{\partial u}{\partial y} \frac{\partial^2 u}{\partial x \partial y} + v \frac{\partial^3 u}{\partial y^3} \right) \right\} + \frac{1}{\rho_{Thnf}} \left[(1 - c_\infty)(T - T_\infty) \beta \rho_{f\infty} g - (c - c_\infty)(\rho_p - \rho_{f\infty}) g \right] - \frac{\sigma_{Thnf}}{\rho_{Thnf}} B_0^2 u \tag{2}$$

$$\frac{\partial T}{\partial t} + u \frac{\partial T}{\partial x} + v \frac{\partial T}{\partial y} = \alpha_{Thnf} \frac{\partial^2 T}{\partial y^2} + \frac{\mu_{Thnf}}{(\rho c_p)_{Thnf}} \frac{1}{(1+\lambda_2)} \left\{ \left(\frac{\partial u}{\partial y} \right)^2 + \lambda_1 \left(u \frac{\partial u}{\partial y} \frac{\partial^2 u}{\partial x \partial y} + \frac{\partial u}{\partial y} \frac{\partial^2 u}{\partial t \partial y} + v \frac{\partial u}{\partial y} \frac{\partial^2 u}{\partial y^2} \right) \right\} + \varepsilon \left[D_B \frac{\partial c}{\partial y} \frac{\partial T}{\partial y} + \frac{D_T}{T_\infty} \left(\frac{\partial T}{\partial y} \right)^2 \right] \tag{3}$$

$$\frac{\partial C}{\partial t} + u \frac{\partial C}{\partial x} + v \frac{\partial C}{\partial y} = D_B \frac{\partial^2 C}{\partial y^2} + \frac{D_T}{T_\infty} \frac{\partial^2 T}{\partial y^2} \tag{4}$$

Initial and boundary conditions for this system are given by

For the case $t < 0$ we keep $T = T_\infty$ and

$C = C_\infty$ at any value of x, y .

For the case $t \geq 0$ keep we $u = U_e, v = 0, T = T_w$, and $D_B \frac{\partial C}{\partial y} + \frac{D_T}{T_\infty} \frac{\partial C}{\partial y} = 0$ at $y = 0$

For $u \rightarrow 0$ we have, $T \rightarrow T_\infty$ and $C \rightarrow C_\infty$ as $y \rightarrow \infty$ (5)

Where u and v are the x - and y -direction flow velocities, respectively and $\nu_{Thnf}, \mu_{Thnf}, \rho_{Thnf}$ are the ternary hybrid nanofluid kinematic viscosity, ternary hybrid nanofluid dynamic viscosity and ternary hybrid nanofluid density respectively. The symbols g is the gravity and

λ_1 -retardation time, σ_{Thnf} is the ternary hybridnanofluid electrical conductivity, T is the temperature, α_{Thnf} symbolizes ternary hybrid nanofluid thermal diffusivity, B_0 indicates the magnetic field, D_B the coefficient of Brownian diffusion, λ_2 -the proportion of relaxation to retardation times, D_T is the coefficient of thermophoresis diffusion, C and T for concentration and fluid temperature respectively. The following similarity transformation is used to transform the governing equations into a system of nonlinear ordinary differential equations.

$$\psi = (av_f)^{0.5} \tau^{0.5} x f(\tau, \eta), \eta = \left(\frac{a}{v_f}\right)^{0.5} \tau^{-0.5} y,$$

$$\tau = 1 - e^{-at}, u = \frac{\partial \psi}{\partial y}, v = -\frac{\partial \psi}{\partial x}$$

$$\theta(\tau, \eta) = \frac{T-T_\infty}{T_w-T_\infty}, \varphi(\tau, \eta) = \frac{C-C_\infty}{C_\infty} \quad (6)$$

Ternary hybrid nanoparticles were correlated by [29]

$$(\rho c_p)_{Thnf} = \varphi_1(\rho c_p)_1 + \varphi_2(\rho c_p)_2 + \varphi_3(\rho c_p)_3 + (1 - \varphi_1 - \varphi_2 - \varphi_3)(\rho c_p)_f \quad (7)$$

$$(\rho)_{Thnf} = (1 - \varphi_1 - \varphi_2 - \varphi_3)\rho_f + \varphi_1\rho_1 + \varphi_2\rho_2 + \varphi_3\rho_3 \quad (8)$$

$$\mu_{Thnf} = \frac{\mu_f}{(1-\varphi_1)^{2.5}(1-\varphi_2)^{2.5}(1-\varphi_3)^{2.5}}$$

$$(9) \frac{(k)_{Thnf}}{(k)_{hnf}} = \frac{k_1+2k_{hnf}-2\varphi_1(k_{hnf}-k_1)}{k_1+2k_{hnf}+\varphi_1(k_{hnf}-k_1)},$$

$$\frac{(k)_{hnf}}{(k)_{nf}} = \frac{k_2+2k_{nf}-2\varphi_2(k_{nf}-k_2)}{k_2+2k_{nf}+\varphi_2(k_{nf}-k_2)},$$

$$\frac{(k)_{nf}}{(k)_f} = \frac{k_3+2k_f-2\varphi_3(k_f-k_3)}{k_3+2k_f+\varphi_3(k_f-k_3)}. \quad (10)$$

$$\frac{(\sigma)_{Thnf}}{(\sigma)_{hnf}} = \frac{\sigma_1(1+2\varphi_1)-\varphi_{hnf}(1-2\varphi_1)}{\sigma_1(1-\varphi_1)+\sigma_{hnf}(1+\varphi_1)},$$

$$\frac{(\sigma)_{hnf}}{(\sigma)_{nf}} = \frac{\sigma_2(1+2\varphi_2)+\varphi_{nf}(1-2\varphi_2)}{\sigma_2(1-\varphi_2)+\sigma_{nf}(1+\varphi_2)},$$

$$\frac{(\sigma)_{nf}}{(\sigma)_f} = \frac{\sigma_3(1+2\varphi_3)+\varphi_f(1-2\varphi_3)}{\sigma_3(1-\varphi_3)+\sigma_f(1+\varphi_3)}. \quad (11)$$

Using Eqs. (6-11), Eqs. (2), (3), and (4) can be simplified into the following nonlinear ODE:

$$\frac{\mu_{Thnf}}{\mu_f} \frac{\rho_f}{\rho_{Thnf}} \frac{1}{(1+\lambda_2)} [\tau - \beta(1-\tau)] f'''' + \frac{\mu_{Thnf}}{\mu_f} \frac{\rho_f}{\rho_{Thnf}} \frac{\beta}{(1+\lambda_2)} \left[\tau(1-\tau) \frac{\partial f''''}{\partial \tau} - \frac{1}{2}(1-\tau)\eta f^{(iv)} + \tau(f''^2 - ff^{(iv)}) \right] - \tau^2 (f'^2 - ff'') + \frac{\rho_f}{\rho_{Thnf}} \tau^2 \lambda (\theta - Nr\varphi) + \frac{1}{2}(1-\tau)\eta \tau f'' -$$

$$\frac{(\sigma)_{Thnf}}{(\sigma)_f} \frac{\rho_f}{\rho_{Thnf}} \tau^2 H a f' = \tau^2 (1-\tau) \frac{\partial f'}{\partial \tau} \quad (12)$$

$$\frac{(k)_{Thnf}}{(k)_f} \frac{(\rho c_p)_f}{(\rho c_p)_{Thnf}} \frac{1}{Pr} \theta'' + \frac{1}{2} \eta \tau (1-\tau) \theta' + \tau^2 f \theta' + \tau (Nb \theta' \varphi' + Nt \theta'^2) +$$

$$\frac{\mu_{Thnf}}{\mu_f} \frac{(\rho c_p)_f}{(\rho c_p)_{Thnf}} \frac{Ec}{(1+\lambda_2)} \left\{ \tau f''^2 + \beta \left[\tau (f' f''^2 - ff'' f''') \right] - (1-\tau) \left(\frac{1}{2} \eta f'' f'''' - \tau f'' \frac{\partial f''}{\partial \tau} + \frac{1}{2} f''^2 \right) \right\} = \tau^2 (1-\tau) \frac{\partial \theta}{\partial \tau} \quad (13)$$

$$\frac{1}{Sc} \tau \varphi'' + \frac{1}{2} (1-\tau) \eta \tau \varphi' + \tau^2 f \varphi' + \frac{1}{Sc} \frac{Nt}{Nb} \tau \theta''$$

$$= \tau^2 (1-\tau) \frac{\partial \varphi}{\partial \tau} \quad (14)$$

The following is a transformation of the initial and boundary conditions:

$$f(\tau, 0) = 0, \quad f'(\tau, 0) = \theta(\tau, 0) = 1, Nb\varphi'(\tau, 0) + Nt\theta'(\tau, 0) = 0,$$

$$\theta(\tau, \infty) = f'(\tau, \infty) = \varphi(\tau, \infty) = 0 \quad (15)$$

Where $Nb = \frac{\epsilon D_B C_\infty}{\nu}$ is the Brownian motion parameter, $Nt = \frac{\epsilon D_T (T_w - T_\infty)}{T_\infty \nu}$ is Thermophoresis parameter, $Sc = \frac{\nu}{D_B}$ represents the Schmidt number, $Ec = \frac{U_e^2}{C_p (T_w - T_\infty)}$ is the Eckert number, $\lambda = \frac{Gr_x}{Re_x^2}$ is the mixed convection parameter, $pr = \nu \rho c_p / k$ is the Prandtl number, $Re_x = U_e x / \nu$ is the Reynolds number, $Ha = \frac{B_0^2 \sigma}{a \rho}$ is the Hartmann number, $\beta = a \lambda_1$ relates the Deborah number $Nr = \frac{(\rho_p - \rho_{f\infty}) C_\infty}{(1 - C_\infty) \beta (T_w - T_\infty)}$ indicates the buoyancy ratio parameter and $Gr_x = g \beta (T_w - T_\infty) (1 - C_\infty) x^3 / \nu^2$ is the Grashof number.

Skin friction factor and local Nusselt number are given by:

$$C_{fx} = -Re_x^{-0.5} \tau^{-0.5} \frac{1}{1 + \lambda_2} \left\{ (1 + \beta) f''(\tau, 0) - (1 - \tau) \beta \left[\frac{\partial f''(\tau, 0)}{\partial \tau} - \frac{1}{2\tau} f''(\tau, 0) \right] \right\},$$

$$C_f(\tau, 0) = C_{fx} Re_x^{0.5} = -\tau^{-0.5} \frac{1}{1 + \lambda_2} \left\{ (1 + \beta) f''(\tau, 0) - (1 - \tau) \beta \left[\frac{\partial f''(\tau, 0)}{\partial \tau} - \frac{1}{2\tau} f''(\tau, 0) \right] \right\} \quad (16)$$

$$Nu_x = -\frac{x \left(\frac{\partial T}{\partial y} \right)_{y=0}}{(T_w - T_\infty)} = -Re_x^{0.5} \tau^{-0.5} \theta'(\tau, 0),$$

$$Nu(\tau, 0) = Nu_x Re_x^{-0.5} = -\tau^{-0.5} \theta'(\tau, 0) \quad (17)$$

3. Results and Discussion

This particular section is provided to analyze the heat conduction and convection properties on a Jeffrey ternary-hybrid nanofluid flowing vertically towards an unstable surface. Variations in velocity, temperature, concentration, local skin friction, and the Nusselt number are represented in Figures 1-17, and their graphical interpretation is discussed.

Figure 1 indicates the impact of the Eckert number on the temperature distribution. From this, we observed that fluid temperature rises with the Eckert number. Because in reality, with larger numbers of Eckert numbers, the maximum amount of heat energy is moved from a high-temperature to a low-temperature region, resulting in more heat transfer. Hence the temperature profile increases with Eckert number.

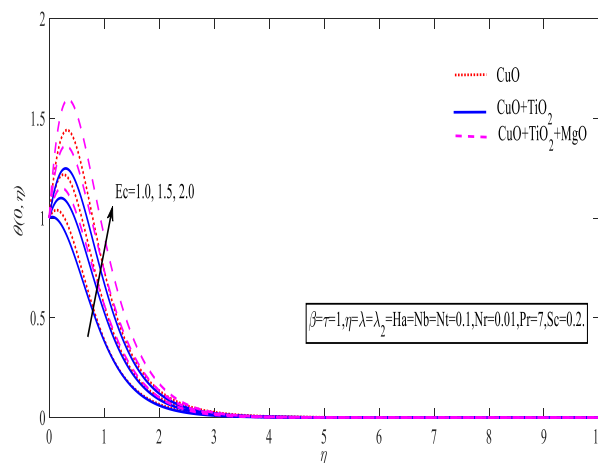


Figure 1: Effect of Eckert number on temperature

The influence of the mixed convection parameter (λ) on the velocities and temperatures is depicted in **Figures 2 and 3**. Flow reveals that higher values of λ are associated with better velocities and slower temperature declines in this case. This is because mixed convection has already taken place when the buoyancy effect on free convection becomes significant. This means that raising the mixed convection parameter value results in higher buoyancy.

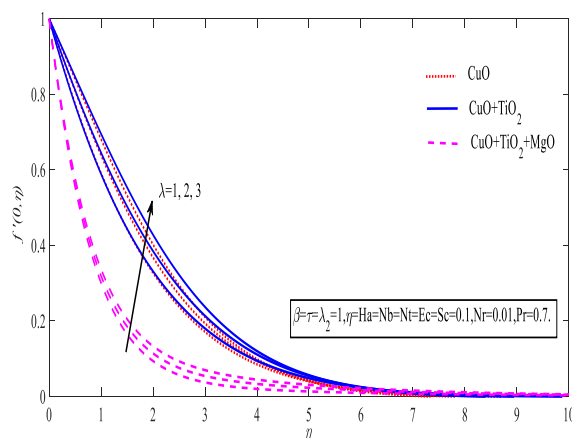


Figure 2: Effect of mixed convection parameter on velocity.

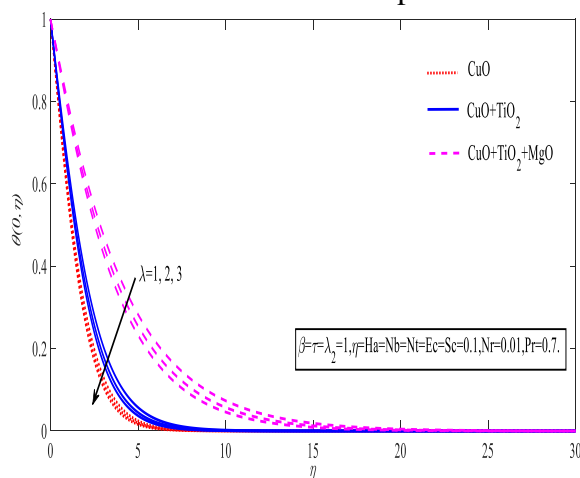


Figure 3: Effect of mixed convection parameter on temperature.

The velocity, temperature, and concentration graphs for various values of the Deborah number are shown in **Figures 4, 5, and 6**. As seen in Figure 4, as increases β , surface friction during surface stretching decreases, causing a corresponding decrease in velocity. In the thermal boundary layer, the temperature distribution improves as β enlarges and the associated thermal boundary layer thickness increases because of a decrease in velocity in the boundary layer. Species concentrations have the same qualitative behaviour as temperatures.

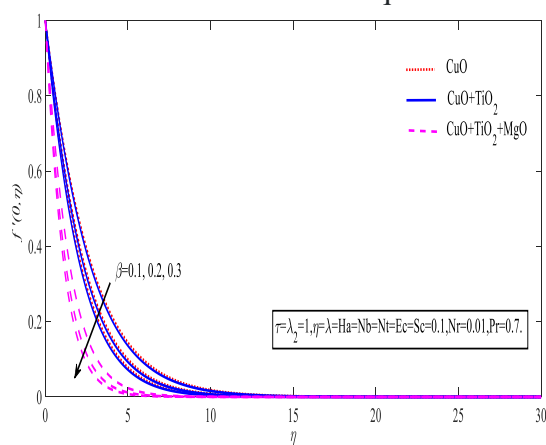


Figure 4: Effect of Deborah number on velocity.

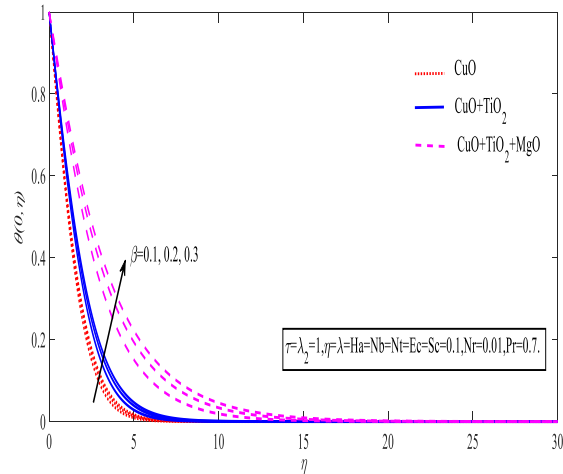


Figure 5: Effect of Deborah's number on temperature.

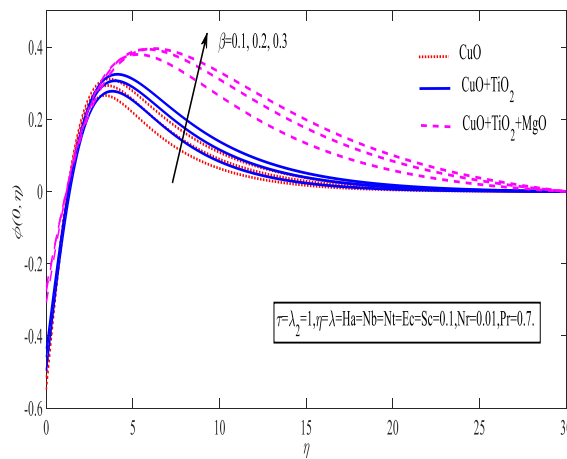


Figure 6: Effect of Deborah number on concentration.

As shown in **Figures 7 and 8**, Ha has the effect of decreasing the boundary layer's average velocity, which causes the layer to become thinner. As can be seen in Figure 8, the temperature profiles rise as Ha gets larger. This graphic shows how the transverse magnetic field makes the thermal boundary layer thicker. This is because the application of a transverse magnetic field causes a body force, such as the Lorentz force, to act against the motion. Therefore, the increased temperature is due to the resistance supplied by this body force to the flow.

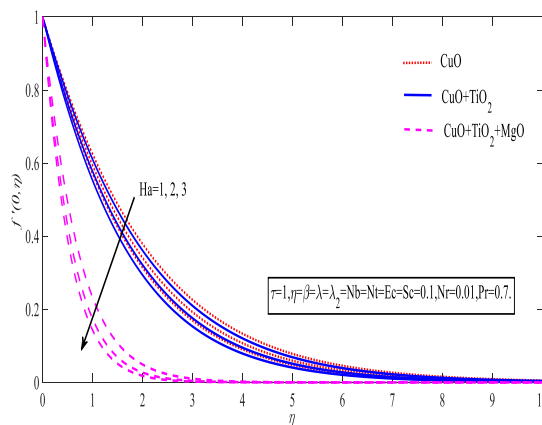


Figure 7: Effect of Hartmann number on velocity.

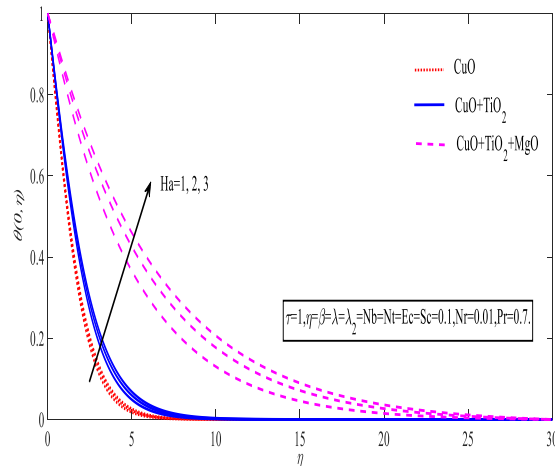


Figure 8: Effect of Hartmann number on temperature.

Figures 9 and 10 show the impact of changing Nt and Nb on the awareness Field separately. As the thermophoresis parameter increases, the boundary layer thickness at the centre of attention increases(Figure 9). Given that $Nt = \frac{\varepsilon D_T (T_w - T_\infty)}{T_\infty \nu}$, the thermophoresis value can be expressed mathematically. An increase in Nt implies that more particles in the fluid are moving from a hotter zone to a cooler zone, increasing the thickness of the convective cooling layer, which is known as the boundary layer. Therefore, as depicted in Figure 9, the attention attributes will be enhanced by an increase in Nt . The Brownian action parameter is reduced by the ternary hybrid nanofluid's nanoparticle concentration. The Brownian motion of particles inside the fluid creates a retarding effect that works against the transferring fluid. eventually, the mass transmission price $\phi(\eta)$ reduces shown in Figure 10.

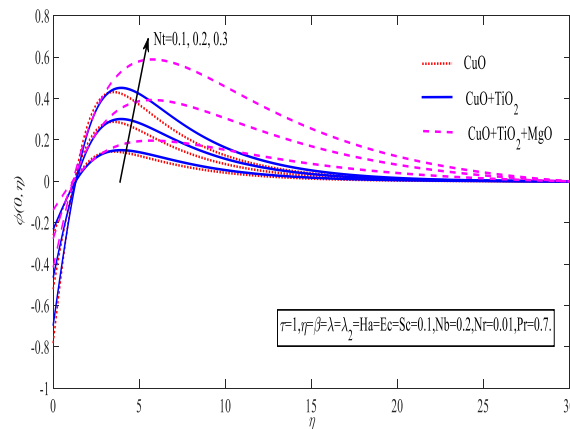


Figure 9:Effect of thermophoresis parameter on concentration.

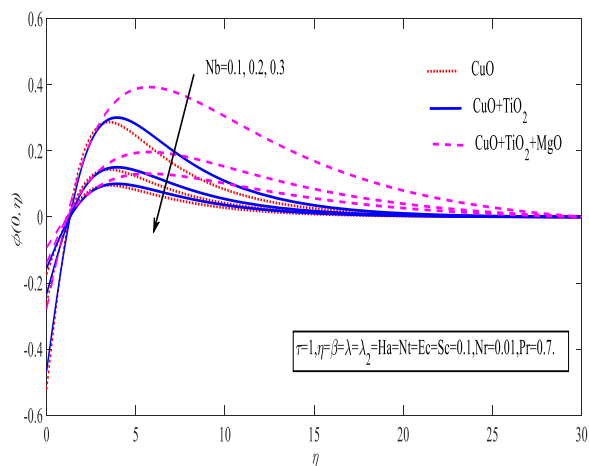


Figure 10: Effect of Brownian motion parameter on concentration.

The impact of Prandtl variation (Pr) on the temperature and concentration distribution is seen in **Figures 11 and 12**. As the Prandtl number rises, the temperature drops quickly. agrees with the physical fact that the effect of a decrease in Prandtl number on the thermal boundary layer of a ternary-hybrid nanofluid is similar to that on the thermal boundary layer of a conventional fluid. An increase in Pr is thought to lower concentration.

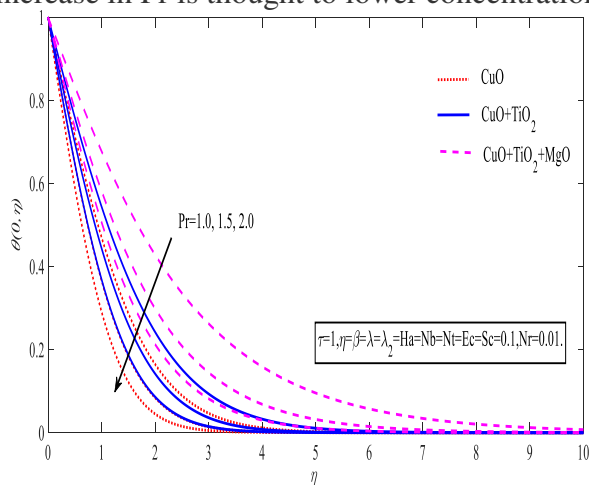


Figure 11: Effect of Prandtl number on temperature

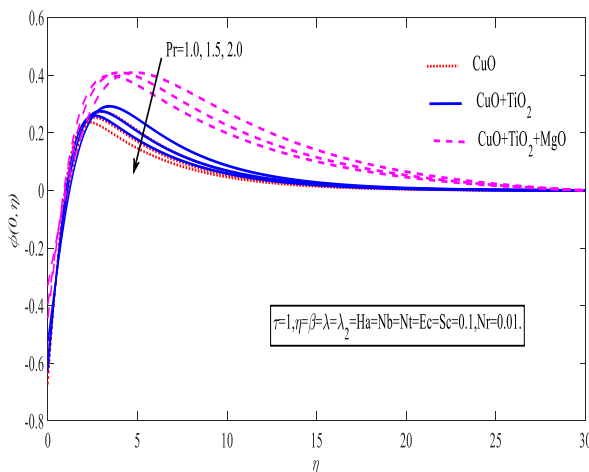


Figure 12: Effect of Prandtl number on concentration

Figure 13 shows the result of analyzing the Schmidt number (Sc) over the concept of the ternary hybrid nanofluid. It is clear from this study that as the Schmidt wide variety Sc is increased in estimation, the concentration of the ternary hybrid nanofluid decreases. The Schmidt number is defined as the ratio of the viscous forces to the mass diffusion forces. When the Schmidt number is increased, the viscous forces of the fluid are amplified while mass diffusion is lowered. Thus, as the mass diffusion is minimized, the fluid's visibility falls.

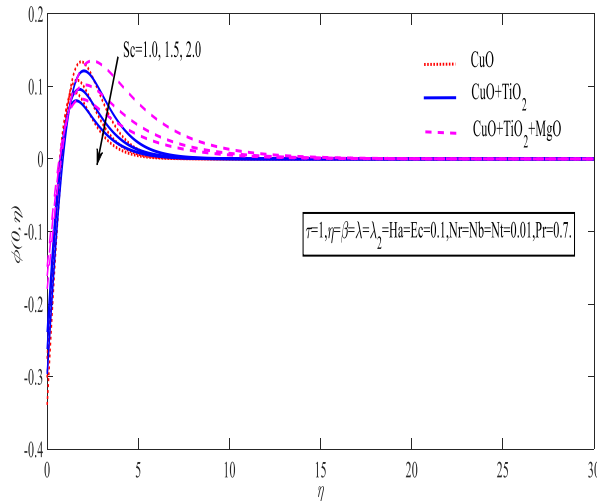


Figure 13: Effect of Schmidt number on concentration.

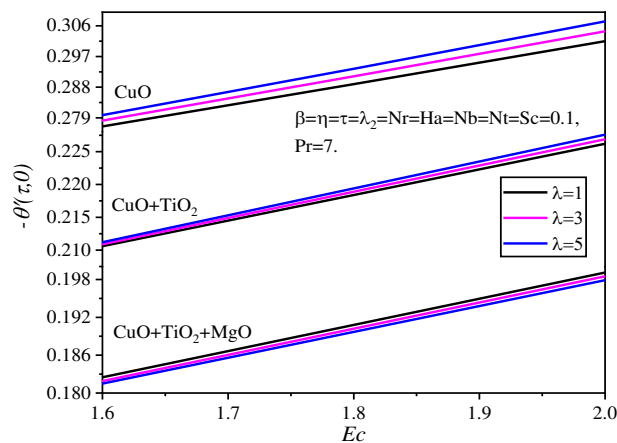


Figure 14: Effect of Eckert number and mixed convection parameter on local Nusselt number.

Figure 14 indicates the Local Nusselt number for the Eckert number vs. the mixed convection parameter. The Eckert number is used for calculating heat dissipation. Improving heat transport requires the use of mixed convection to maximize thermal characteristics. In the cases of CuO-nanoparticles and CuO+ TiO₂-hybrid nanoparticles, the Nusselt number rises as the mixed convection parameter is raised to higher values. Because of the higher thermal conduction of the created hybrid nanofluid, its heat transmission performance is improved. Specifically, if CuO + TiO₂ + MgO-ternary nanoparticles, the Nusselt number is reduced because the thermal conduction of the third nanoparticle is lower than that of copper and aluminium.

Figure 15 shows the Skin friction for the Eckert number vs. the mixed convection parameter. Specifically, if CuO-nanoparticles, the skin friction value reduces when raising the values λ ,

whereas the skin friction (C_f) value increases with adding nanoparticles and enhancing the fluid density in the case of CuO+ TiO₂ -hybrid nanoparticles and CuO+ TiO₂ + MgO-ternary nanoparticles.

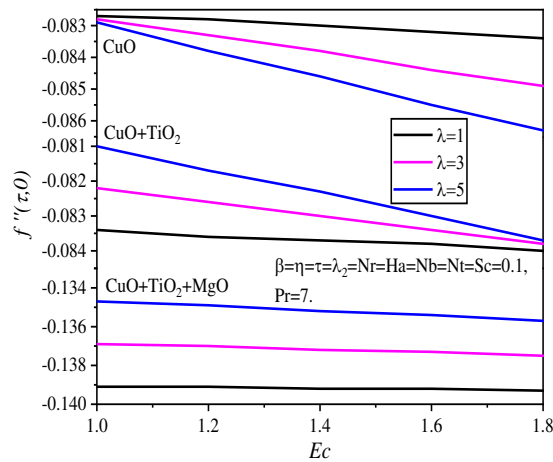


Figure 15: Effect of Eckert number and mixed convection parameter on skin friction.

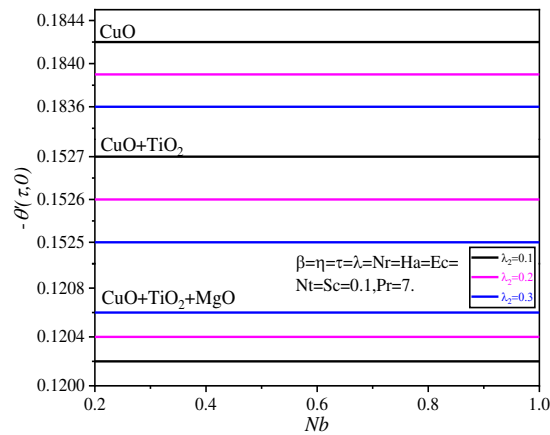


Figure 16: Effect of Brownian motion parameter and the ratio of relaxation to retardation times on local Nusselt number.

Figure 16 shows how the local Nusselt number varies as a function of the Brownian motion parameter and the relaxation-to-retardation time ratio. The rate of heat transmission decreases for nanoparticles and hybrid nanoparticles and it is increased for ternary hybrid nanoparticles as larger values of. Adding more nanoparticles to a fluid causes the particles to flow more quickly and efficiently, which boosts the heat conduction of the fluid and, in turn, raises the fluid's temperature.

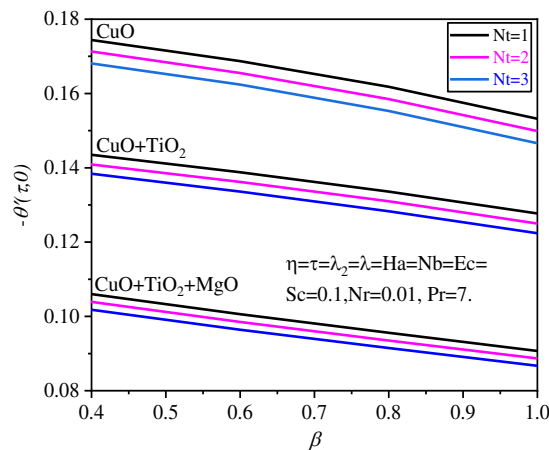


Figure 17: Effect of thermophoresis parameter and Deborah number on local Nusselt number.

Figure 17 shows how the local Nusselt number changes depending on the thermophoresis parameter and the Deborah number. whereas the thermophoresis (Nt) strength causes the ternary hybrid nanoparticles to transport the hotter region to the colder region, This causes the thermal boundary layer to thicken, the Nusselt value has decreased as Nt has increased. In rheology, materials' fluidity is described by their Deborah number (β), which is calculated under controlled flow circumstances. Furthermore, a larger increase parallels a notable decrease in Nu . This is because an increase in the Deborah number (β) indicates an elastically solid material, lowering the Nusselt number, whereas a decrease in the Deborah number indicates a vicious impact relative to the elastic impact.

4. Conclusions

Thermophoresis is used to investigate the effect of Brownian motion (Nb) and viscous dissipation on the mixed convection flow of a Jeffrey ternary hybrid nanofluid via a fluctuating surface. A ternary hybrid nanofluid is created when three distinct types of nanoparticles are mixed with the base fluid. Since the highest derivative term contains a singularity, the governing equations are transformed using a transformation of similarity to yield a set of PDEs that are sensitive to the initial conditions; the numerical solution is obtained using a fourth-order R.K. integration scheme and shooting methods, the outcomes of these numeric calculations are illustrated graphically and discussed in detail for a range of input values.

- Deborah's number and Hartmann's number both decreased, whereas higher values of the mixed convection parameter increased the velocity profile.
- There has been an improvement in thermal properties as measured by the Eckert number (Ec), Deborah number (β), and the Hartmann number (Ha), and its decline as measured by the mixed convection parameters (λ).
- As the Brownian motion factor has increased in value, mass diffusion has decreased, but thermophoresis and the Deborah number have increased in mass diffusion.
- Brownian motion increased the Nusselt value, but thermophoresis and the Eckert number both decreased it.
- The increased effective motion of the particle due to Brownian motion also increases the thermal conductivity of the fluid, which in turn raises the fluid temperature.

- This study concludes that ternary hybrid nanofluids have a greater thermal flow rate than either hybrid or nanofluids.
- A higher Eckert number indicates higher fluid density, which in turn increases the skin friction value.
- When the Prandtl and Schmidt numbers are increased, the temperature and concentration distributions are flattened.

References

- [1] E. El-Zahar, A. Rashad, and L. Seddek, "Impacts of Viscous Dissipation and Brownian motion on Jeffrey Nanofluid Flow over an Unsteady Stretching Surface with Thermophoresis," *Symmetry (Basel)*, vol. 12, no. 9, p. 1450, Sep. 2020, doi: 10.3390/sym12091450.
- [2] R. Ali, A. Shahzad, K. us Saher, Z. Elahi, and T. Abbas, "The thin film flow of Al₂O₃ nanofluid particle over an unsteady stretching surface," *Case Stud. Therm. Eng.*, vol. 29, p. 101695, Jan. 2022, doi: 10.1016/j.csite.2021.101695.
- [3] H. Ş. Aybar, M. Sharifpur, M. R. Azizian, M. Mehrabi, and J. P. Meyer, "A Review of Thermal Conductivity Models for Nanofluids," *Heat Transf. Eng.*, vol. 36, no. 13, pp. 1085–1110, Sep. 2015, doi: 10.1080/01457632.2015.987586.
- [4] N. S. Akbar, "A New Thermal Conductivity Model With Shaped Factor Ferromagnetism Nanoparticles Study for the Blood Flow in Non-Tapered Stenosed Arteries," *IEEE Trans. Nanobioscience*, vol. 14, no. 7, pp. 780–789, Oct. 2015, doi: 10.1109/TNB.2015.2462755.
- [5] N. S. Akbar and Z. H. Khan, "Effect of variable thermal conductivity and thermal radiation with CNTS suspended nanofluid over a stretching sheet with convective slip boundary conditions: Numerical study," *J. Mol. Liq.*, vol. 222, pp. 279–286, Oct. 2016, doi: 10.1016/j.molliq.2016.06.102.
- [6] N. S. Akbar, D. Tripathi, Z. H. Khan, and O. A. Bég, "A numerical study of magnetohydrodynamic transport of nanofluids over a vertical stretching sheet with exponential temperature-dependent viscosity and buoyancy effects," *Chem. Phys. Lett.*, vol. 661, pp. 20–30, Sep. 2016, doi: 10.1016/j.cplett.2016.08.043.
- [7] N. S. Akbar and M. T. Mustafa, "Ferromagnetic effects for nanofluid venture through composite permeable stenosed arteries with different nanosize particles," *AIP Adv.*, vol. 5, no. 7, p. 077102, Jul. 2015, doi: 10.1063/1.4926342.
- [8] N. S. Akbar, D. Tripathi, and O.A. Beg, "Modeling Nanoparticle Geometry effects on peristaltic pumping of medical magnetohydrodynamic nanofluids with heat transfer," *J. Mech. Med. Biol.*, vol. 16, no. 06, p. 1650088, Sep. 2016, doi: 10.1142/S0219519416500883.
- [9] M. Ahmad, T. Muhammad, I. Ahmad, and S. Aly, "Time-dependent 3D flow of viscoelastic nanofluid over an unsteady stretching surface," *Phys. A Stat. Mech. its Appl.*, vol. 551, p. 124004, Aug. 2020, doi: 10.1016/j.physa.2019.124004.
- [10] F. Hussain, A. Hussain, and S. Nadeem, "Unsteady shear-thinning behaviour of nanofluid flow over exponential stretching/shrinking cylinder," *J. Mol. Liq.*, vol. 345, p. 117894, Jan. 2022, doi: 10.1016/j.molliq.2021.117894.
- [11] Y.-X. Li *et al.*, "Simultaneous features of Wu's slip, nonlinear thermal radiation and activation energy in unsteady bio-convective flow of Maxwell nanofluid configured by a stretching cylinder," *Chinese J. Phys.*, vol. 73, pp. 462–478, Oct. 2021, doi: 10.1016/j.cjph.2021.07.033.
- [12] J. Liu *et al.*, "Thermal analysis of a radiative slip flow of an unsteady casson nanofluid toward a stretching surface subject to the convective condition," *J. Mater. Res. Technol.*, vol. 15, pp. 468–476, Nov. 2021, doi: 10.1016/j.jmrt.2021.08.045.

- [13] W. A. Khan, J. R. Culham, and O. D. Makinde, "Combined heat and mass transfer of third-grade nanofluids over a convectively-heated stretching permeable surface," *Can. J. Chem. Eng.*, vol. 93, no. 10, pp. 1880–1888, Oct. 2015, doi: 10.1002/cjce.22283.
- [14] N. Freidoonimehr, M. M. Rashidi, and S. Mahmud, "Unsteady MHD free convective flow past a permeable stretching vertical surface in a nano-fluid," *Int. J. Therm. Sci.*, vol. 87, pp. 136–145, Jan. 2015, doi: 10.1016/j.ijthermalsci.2014.08.009.
- [15] H. Babar and H. M. Ali, "Towards hybrid nanofluids: Preparation, thermophysical properties, applications, and challenges," *J. Mol. Liq.*, vol. 281, pp. 598–633, May 2019, doi: 10.1016/j.molliq.2019.02.102.
- [16] J. Sarkar, P. Ghosh, and A. Adil, "A review on hybrid nanofluids: Recent research, development and applications," *Renew. Sustain. Energy Rev.*, vol. 43, pp. 164–177, Mar. 2015, doi: 10.1016/j.rser.2014.11.023.
- [17] A. Wakif, A. Chamkha, T. Thumma, I. L. Animasaun, and R. Sehaqui, "Thermal radiation and surface roughness effects on the thermo-magneto-hydrodynamic stability of alumina–copper oxide hybrid nanofluids utilizing the generalized Buongiorno's nanofluid model," *J. Therm. Anal. Calorim.*, vol. 143, no. 2, pp. 1201–1220, Jan. 2021, doi: 10.1007/s10973-020-09488-z.
- [18] N. A. Che Sidik, M. Mahmud Jamil, W. M. A. Aziz Japar, and I. Muhammad Adamu, "A review on preparation methods, stability and applications of hybrid nanofluids," *Renew. Sustain. Energy Rev.*, vol. 80, pp. 1112–1122, Dec. 2017, doi: 10.1016/j.rser.2017.05.221.
- [19] H. W. Xian, N. A. C. Sidik, and R. Saidur, "Impact of different surfactants and ultrasonication time on the stability and thermophysical properties of hybrid nanofluids," *Int. Commun. Heat Mass Transf.*, vol. 110, p. 104389, Jan. 2020, doi: 10.1016/j.icheatmasstransfer.2019.104389.
- [20] I. Kazemi, M. Sefid, and M. Afrand, "A novel comparative experimental study on rheological behavior of mono & hybrid nanofluids concerned graphene and silica nano-powders: Characterization, stability and viscosity measurements," *Powder Technol.*, vol. 366, pp. 216–229, Apr. 2020, doi: 10.1016/j.powtec.2020.02.010.
- [21] F. Soltani, D. Toghraie, and A. Karimipour, "Experimental measurements of thermal conductivity of engine oil-based hybrid and mono nanofluids with tungsten oxide (WO₃) and MWCNTs inclusions," *Powder Technol.*, vol. 371, pp. 37–44, Jun. 2020, doi: 10.1016/j.powtec.2020.05.059.
- [22] X. Sun, I. L. Animasaun, K. Swain, N. A. Shah, A. Wakif, and P. O. Olanrewaju, "Significance of nanoparticle radius, inter-particle spacing, inclined magnetic field, and space-dependent internal heating: The case of chemically reactive water conveying copper nanoparticles," *ZAMM - J. Appl. Math. Mech. / Zeitschrift für Angew. Math. und Mech.*, vol. 102, no. 4, Apr. 2022, doi: 10.1002/zamm.202100094.
- [23] A. S. Sabu, A. Wakif, S. Areekara, A. Mathew, and N. A. Shah, "Significance of nanoparticles' shape and thermo-hydrodynamic slip constraints on MHD alumina-water nanoliquid flows over a rotating heated disk: The passive control approach," *Int. Commun. Heat Mass Transf.*, vol. 129, p. 105711, Dec. 2021, doi: 10.1016/j.icheatmasstransfer.2021.105711.
- [24] A. Dawar, A. Wakif, T. Thumma, and N. A. Shah, "Towards a new MHD non-homogeneous convective nanofluid flow model for simulating a rotating inclined thin layer of sodium alginate-based Iron oxide exposed to incident solar energy," *Int. Commun. Heat Mass Transf.*, vol. 130, p. 105800, Jan. 2022, doi: 10.1016/j.icheatmasstransfer.2021.105800.
- [25] W. Cao, A. I.L., S.-J. Yook, O. V.A., and X. Ji, "Simulation of the dynamics of a colloidal mixture of water with various nanoparticles at different levels of partial slip:

- Ternary-hybrid nanofluid,” *Int. Commun. Heat Mass Transf.*, vol. 135, p. 106069, Jun. 2022, doi: 10.1016/j.icheatmasstransfer.2022.106069.
- [26] S. Manjunatha, V. Puneeth, B. J. Gireesha, and A. J. Chamkha, “Theoretical Study of Convective Heat Transfer in Ternary Nanofluid Flowing past a Stretching Sheet,” *J. Appl. Comput. Mech.*, vol. 8, no. 4, pp. 1279–1286, 2022, doi: 10.22055/JACM.2021.37698.3067.
- [27] A. F. I. Jalal Mohammed Zayan¹, Abdul Khaliq Rasheed^{2*}, Akbar John³, Mohammed Khalid⁴, “Experimental Investigation on Rheological Properties of Water Based Novel,” 2021.
- [28] M. Arif, P. Kumam, W. Kumam, and Z. Mostafa, “Heat transfer analysis of radiator using differently shaped nanoparticles water-based ternary hybrid nanofluid with applications: A fractional model,” *Case Stud. Therm. Eng.*, vol. 31, p. 101837, Mar. 2022, doi: 10.1016/j.csite.2022.101837.
- [29] F. Mebarek-Oudina, R. Fares, A. Aissa, R. W. Lewis, and N. H. Abu-Hamdeh, “Entropy and convection effect on magnetized hybrid nano-liquid flow inside a trapezoidal cavity with the zigzagged wall,” *Int. Commun. Heat Mass Transf.*, vol. 125, p. 105279, Jun. 2021, doi: 10.1016/j.icheatmasstransfer.2021.105279.